nature research

https://doi.org/10.1038/s41563-020-0768-7

Supplementary information

A natural impact-resistant bicontinuous composite nanoparticle coating

In the format provided by the authors and unedited

Supplementary information for

A natural impact resistant bi-continuous composite nanoparticle coating

Wei Huang[1,2], Mehdi Shishehbor[3], Nicolás Guarín-Zapata[3], Nathan D. Kirchhofer[4], Jason Li[4], Luz Cruz[5], Taifeng Wang[5], Sanjit Bhowmick[6], Douglas Stauffer[6], Praveena Manimunda[6], Krassimir N. Bozhilov[7], Roy Caldwell[8], Pablo Zavattieri[3], David Kisailus[1,2,5]*

[1]Department of Chemical and Environmental Engineering, University of California, Riverside, CA, 92521

[2]Department of Materials Science and Engineering, University of California, Irvine, CA, 92697

[3]Lyles School of Civil Engineering, Purdue University, West Lafayette, IN 47907

[4]Oxford Instruments Asylum Research, Goleta, CA, 93117

[5]Materials Science and Engineering Program, University of California, Riverside, CA, 92521

[6]Bruker, Minneapolis, MN, 55344

[7]Central Facility for Advanced Microscopy and Microanalysis, University of California, Riverside, CA, 92521

[8]Department of Integrative Biology, University of California, Berkeley, CA, 94720

*Correspondence to: david.k@uci.edu

Supplementary Discussion

Organic phase percentage in impact surface

Based on TEM and AFM analyses, the volume fraction of the organic phase within these particles was determined to be ~ 44±10 vol% (Supplementary Figure 3). This value is slightly higher than that determined from thermogravimetric analysis (i.e., ~ 17 wt% or ~ 32.7 vol%). This difference is likely due to the fact that the TGA data was calculated based on the assumption that the average density of the organic components is 1.35 g/cm3 (like that reported for proteins), whereas the density of the actual organic phase, which is hydrated, is likely lower [1].

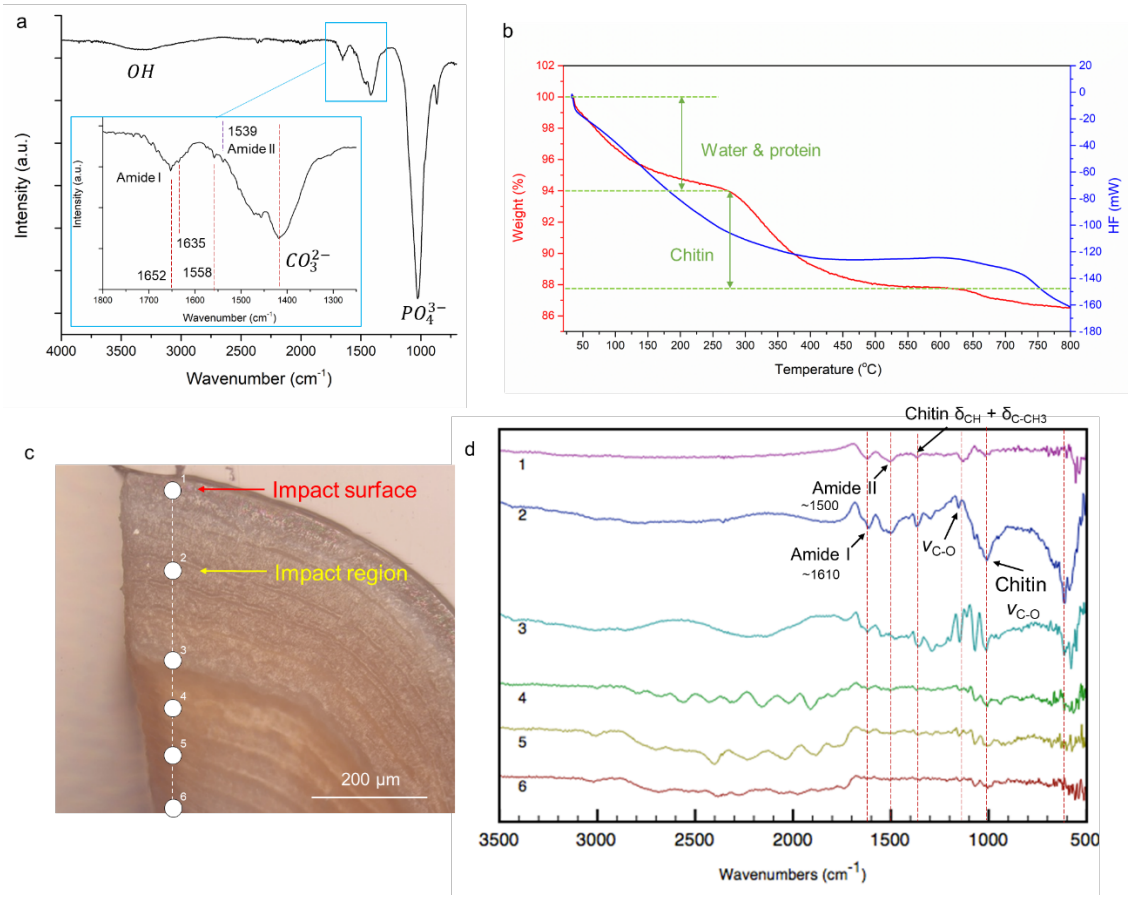

Supplementary Figure 1. FTIR and TGA characterization of nanoparticles on the impact surface. (a) FTIR spectrum of the nanoparticles on the impact surface, indicating the existence of hydroxyapatite, chitin and protein. (b) TGA/DSC curves of the HAP nanoparticles. The weight percentage of the organics, including chitin and protein, is ~ 12 %. (c) Optical micrograph of demineralized dactyl club. The white dots represent different regions where FTIR spectra were acquired. (d) FTIR spectra from regions indicated by the white dots in (c). Amide I, amide II and C-O stretching peaks are indicated in the spectrum 1 and 2, showing the existence of chitin. The amide I and II bands shift to a lower wavenumber compared with chitin amide bands (amide I 1630~1660 cm^{-1}, amide II ~1558 cm^{-1}), which are more characteristic of proteins.

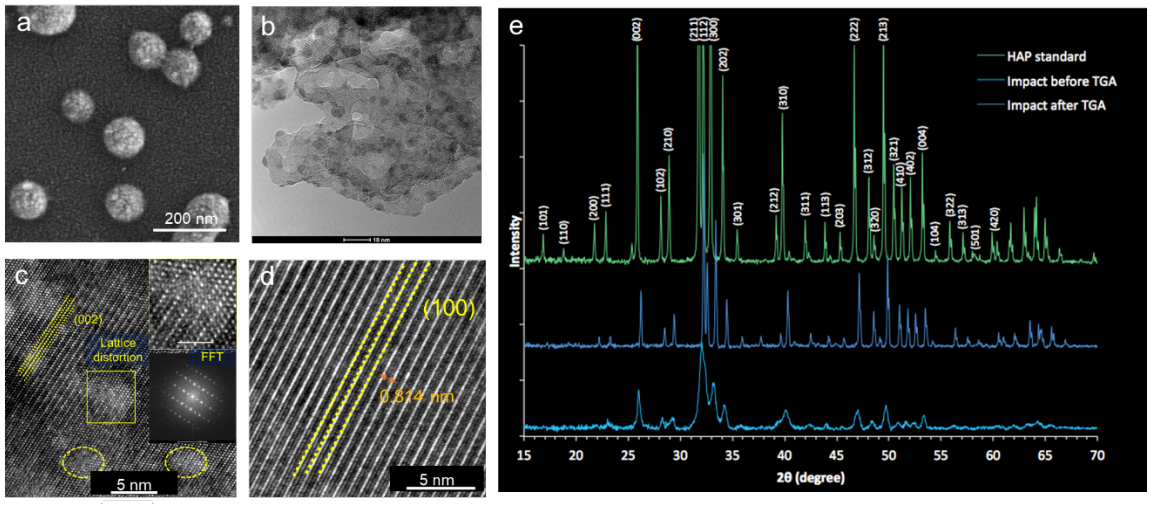

Supplementary Figure 2. (a) TEM of HAP nanoparticles after TGA. (b) HRTEM of HAP nanoparticles on the impact surface after staining with uranyl acetate and lead citrate. The HAP continuous network is revealed. The darker regions are proteins revealed from staining. (c) HRTEM of (002) planes within a single secondary particle. The areas of lighter contrast are marked with yellow ellipses to highlight regions containing organic, with distorted crystal planes. The inset yellow box shows a higher magnification of the distorted lattice. Scale bar is 2 nm. (d) HRTEM of (100) HAP crystal planes. No lattice distortion is observed (as compared to particles in (c)). Three independent dactyl clubs from 3 different mantis shrimps were examined. Similar results as shown in (a-d) were observed. (e) XRD of particles scratched from the impact surface and impact region. The broader diffraction peaks from the native sample (before TGA) narrowed due to grain growth during annealing. HAP appears stable, with no secondary phase formation, even after heating to 800 ºC in air.

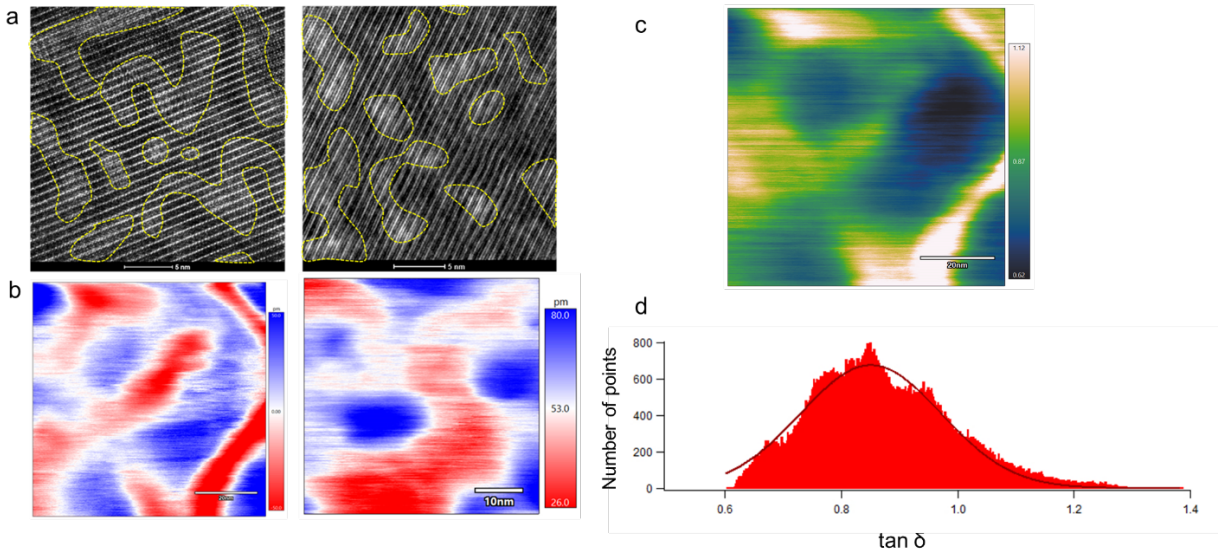

Supplementary Figure 3. TEM and AFM images highlighting the bi-continuous network of inorganic and organic phases. The yellow circles in the top two HRTEM images (a) highlight the organic networks, which shows a lower contrast in TEM. (b) AFM images at the bottom are indentation depth maps. The indentation depth is larger in the area where organics are present because of a lower stiffness. Thus, the blue areas are organic, while the red color represents the hydroxyapatite network. (c) AFM mapping of tan δ of the nanoparticles. (d) Distribution of the values of tan δ in the nanoparticle. TEM and AFM of three independent dactyl clubs from three different mantis shrimps show similar bi-continuous networks.

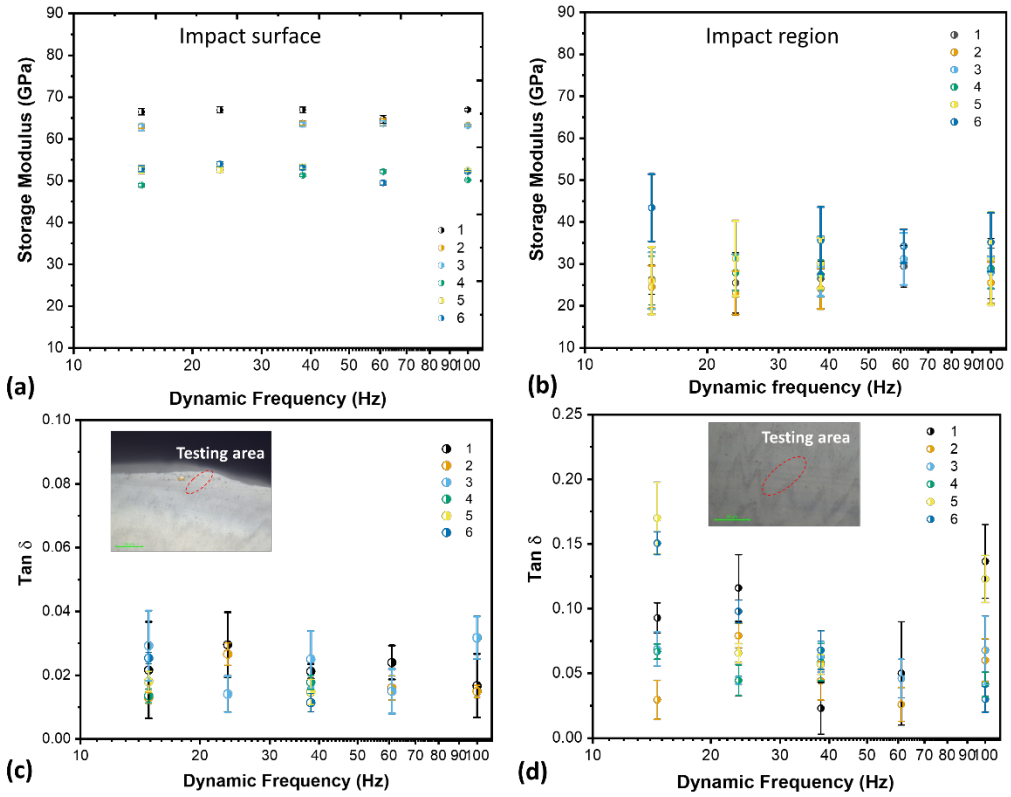

Supplementary Figure 4. NanoDMA of impact surface and impact regions. Storage modulus and tan δ were acquired as a function of frequency (9 – 100 Hz). The large variations of modulus and tan δ in the impact region are due to the different fiber orientations. In the nanoDMA tests, n=6 independent locations were tested within two different biological independent samples. Data are presented as mean values +/- standard deviation.

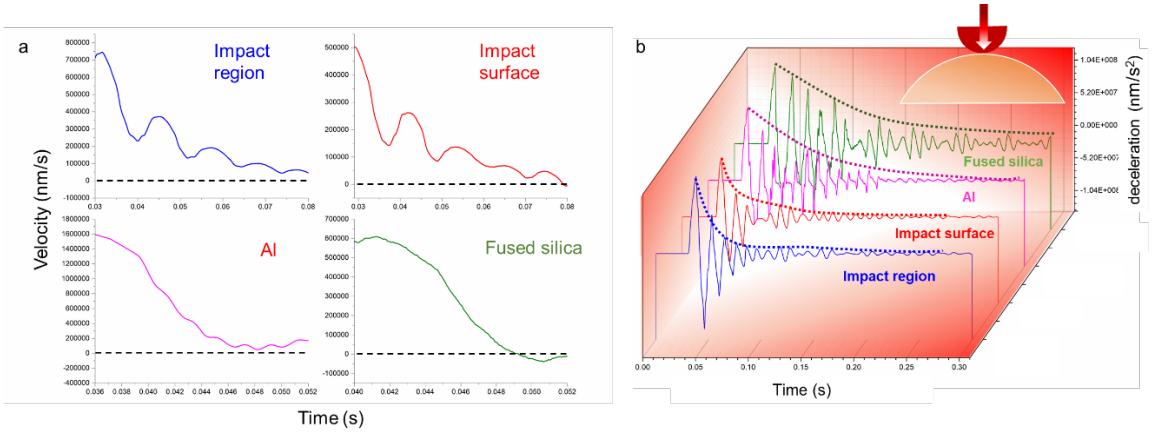

Supplementary Figure 5. (a) Velocity of the indenter head as a function of time during micro-impact tests. The time frame of the impact velocity decreasing from its peak value to zero on the impact surface is ~ 50 ms, which is much larger than that in Al (~12 ms) and fused silica (~8 ms), indicating better damping properties in the impact region and impact surface. (b) Plots of deceleration as a function of time during the impact tests in the impact region and impact surface. Single crystal Al and fused silica are tested for comparison. The deceleration in both the impact surface and the impact region are larger than in those in Al and fused silica, indicating a more significant damping behavior in the dactyl club.

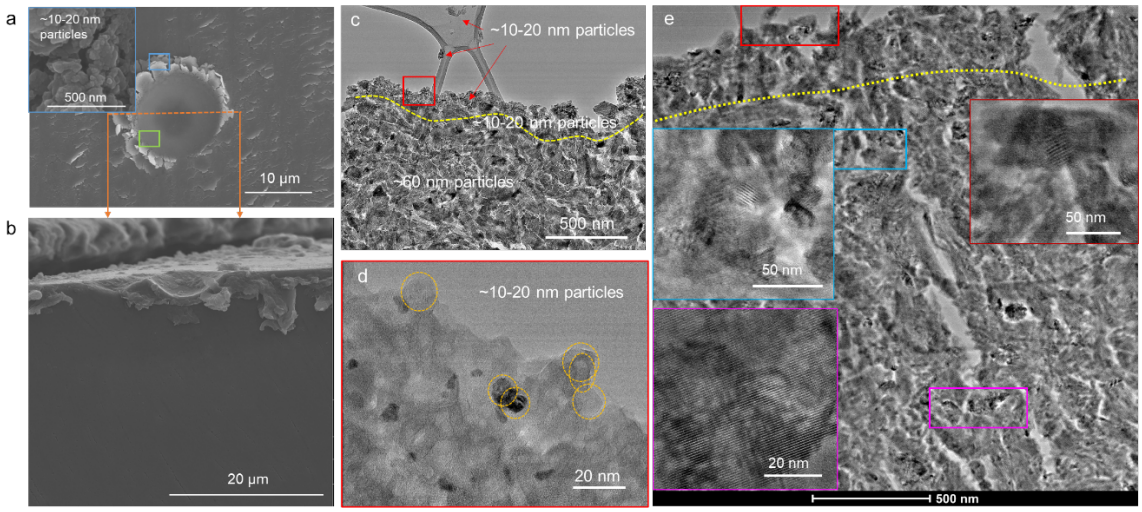

Supplementary Figure 6. SEM and TEM images of damage within the impact surface after a single high strain rate micro-impact. (a) SEM images of the damage area after impact tests. The inset image shows particle size ~10 - 20 nm, indicating particle breakages after impacts. (b) SEM image of the transverse section of the impact location. No obvious damage or cracks are observed underneath the impact area. (c) and (d) TEM images indicating the large secondary particles are broken into ~ 10-20 nm primary particles after high strain rate impacts. (e) Damage at different depths from the surface. The particle breakage is limited to ~100 – 200 nm depth from the impact surface. The particle breakage area is indicated with a yellow dashed line. Dislocation and amorphization are found in the red and blue boxed areas, but not in the purple area, indicating impact induced dislocation and amorphization is limited to ~1000 nm depth from the surface. Damage modes acquired with SEM and TEM from three independent dactyl club samples are similar.

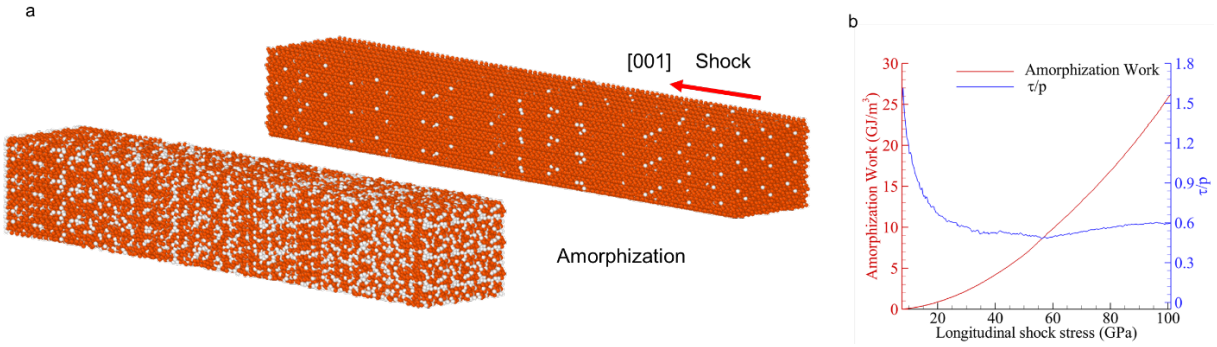

Supplementary Figure 7. MD simulation of shock induced amorphization in HAP crystals. (a) MD models of shock wave along [001] direction of HAP crystals. White dots indicate amorphization areas. (b) Amorphization work as a function of longitudinal shock stress. The impact stress in the current impact tests is ~0.98 GPa, leading to a ~0.038 GJ/m^3 amorphization work. τ represents shear stress, p is the hydrostatic pressure.

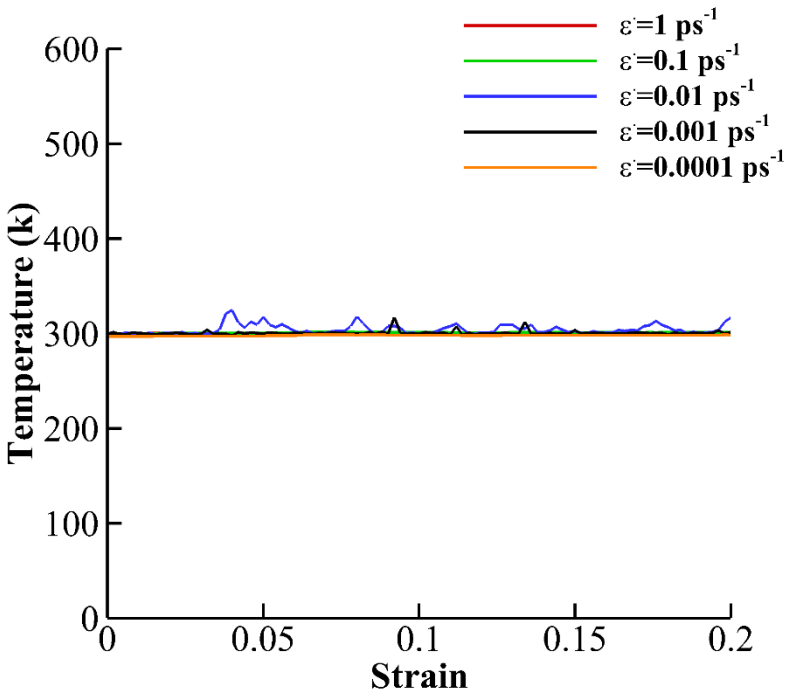

Supplementary Figure 8. Plot of temperature as a function of strain, indicating thermal stability (i.e., maintained at approximately room temperature, 300 K) when loaded at different strain rates.

Supplementary Video 1. HAP nanoparticles at different tilt angles in TEM.

Supplementary Video 2. *In-situ* compression of a HAP nanoparticle.

Supplementary References

1. Fischer, H., Polikarpov, I. & Craievich, A. F. Average protein density is a molecular-weight-dependent function. Protein Science 13, 2825-2828 (2004).

Supplementary source data 1. Source data for Figure 3h-j.

Supplementary source data 2. Source data for Figure 5j.

Supplementary source data 3. Source data for Figure 6e, f.

Supplementary source data 4. Source data for Extended Data Figure 3a, b.

Supplementary source data 5. Source data for Extended Data Figure 4e.